Ultrashort pulse polarization control in silicon waveguides

Montasir Qasymeh, Sergey A. Ponomarenko, and Michael Cada

Department of Electrical and Computer Engineering
Dalhousie University, Halifax, NS, B3J 2X4, Canada

montasir@dal.ca

Abstract: The nonlinear polarization dynamics of ultrashort optical pulses propagating in a low birefringent silicon waveguide is theocratically and numerically studied, with a static electric field applied across the waveguide. It is shown that the pulse shape and polarization evolution can be efficiently controlled by adjusting the magnitude of the applied dc field. It is also demonstrated that the polarization instability regime can be achieved in such waveguides – despite the presence of strong linear losses – by appropriately engineering the spatial distribution of the control field along the waveguide. The simulations indicate that short silicon waveguides can serve as a viable platform for developing re-configurable all-optical and/or optically assisted electro-optic devices in the spectral range spanning from near- to mid-infrared.

OCIS codes: (190.3270) Kerr effect; (250.4390) Nonlinear optics, integrated optics; (190.5970) Semiconductor nonlinear optics including MQW.

References and links

1. B. Jalali, "Can silicon change photonics?", Phys. Status Solidi A, **2,** 213–224 (2008).
2. G. T. Reed, "Optical age of silicon" Nature **427,** 595–596(2004).
3. L. Pavesi, "Will silicon be the photonic material of the third millennium?" J.Phys.: Condens. Matter **15,** R1169–R1196 (2003).
4. Q. Lin, Oskar J. Painter, and G. P. Agrawal, "Nonlinear optical phenomena in silicon waveguides: modeling and applications ," Opt. Express **15,** 16604–16644 (2007).
5. R. Dekker, N. Usechak, M, Forst, and A. Driessen, "Ultrafastnonlinear all-optical processes in silicon-on-insulator waveguides," J. Phys. D: Appl.Phys.**40**, R249–R271 (2007).
6. C. Manolatou and M. Lipson, " All-optical silicon modulators based on carrier injection by two-photon absorption," IEEE J. Lightwave Technol, **24,** 1433–1439 (2006).
7. T. K. Liang, L. R. Nunes, M. Tsuchiya, K. S. Abedin, T. Miyazaki, D. Van Thourhout, W. Bogaerts, P. Dumon, R. Baets, and H. K. Tsang, "High speed logic gate using two-photon absortption in silicon wavegiudes," Opt. Commun. **265,** 171–174 (2006).
8. R. Dekker, A. Driessen, T. Wahlbrink, C. Moormann, J. Niehusmaan, and M. Forst, " Ultrafast Kerr-induced all-optical wavelength conversion in silicon waveguides using 1.55 femtosecond pulses," Opt. Express **14,** 8336–8346 (2006).
9. V. Raghunathan, R. Claps, D.Dimitropoulos, and B. Jalali, " Parametric Raman wavelength conversion in scaled silicon waveguides," IEEE J.Lightwave Technol, **23,** 2094–2102 (2005).
10. R. Claps, D. Dimitropoulos, V. Raghunathan,Y. Han, and B. Jalali,"Observation of stimulated Raman amplification in silicon waveguides," Opt. Express **11,** 1731–1739 (2003).
11. M. A. Forst , A. C. Turner, J. E. Sharping, B. S. Schmidt, M. Lipson, and A. L. Gaeta, " Broad-band optical parametric gain on a silicon photonic chip," Nature **441,** 960–963 (2006).
12. H. Rong, R. Jones, A. Liu, O. Cohen, D. Hak, A. Fang, and M. Paniccia, "A continuous-wave Raman silicon laser," Nature **433,** 725–728 (2005).
13. T. J. Kippenberg, S. M. Spillane, D. K. Armani, and K. J. Vahala, "Ultralow-threshold microcavity Raman laser on a microelectronic chip," Opt. Lett. **29,** 1224–1227 (2004).

#102344 - $15.00 USD Received 6 Oct 2008; revised 12 Dec 2008; accepted 17 Dec 2008; published 29 Jan 2009

14. L. Yin, Q.Lin, and G. P. Agrawal, "Soliton fission and suprercontinuum generation in silicon waveguides," Opt. Lett.**32,** 391–393 (2007).
15. J. Zhang, Q. Lin, G. Piredda, R. W. Boyd, G. P. Agrawal, and P. M. Fuachet, "Optical solitons in a silicon waveguide," Opt. Express **15,** 7682–7688 (2007).
16. V. M. N. Passaro and F. De Leonardis, "Solitons in SOI optical waveguides," Adv. Studies Theor. Phys., **2,** 769–785 (2008).
17. M. Li, S. A. Ponomarenko, M. Qasymeh, and M. Cada, "Electronic control of soliton power transfer in silicon nanocrystal," Opt. Express **16,** 9587–9594 (2008).
18. M. Cada, M. Qasymeh, and J. Pistora, "Electrically and optically controlled cross-polarized wave conversion," Opt. Express **16,** 3083–3100 (2008).
19. H. G. Winful, "Self-induced polarization changes in birefringent optical fibers ," Appl.Phys.Lett. **47,** 213–215 (1985).
20. G. P. Agrawal,"Nonlinear fiber optics," 4th ed. (Academic Press, Boston, 2007).
21. J. Zhang, Q. Lin, G. Piredda, R. W. Boyd, G. P. Agrawal, and P. M. Fauchet, "Anisotropic nonlinear response of silicon in the near-infrared region," Appl. Phys. Lett. **90,** 071113 (2007).
22. R. Salem and T. E. Murphy, "Polarization-insensitive cross correlation using two-photon absorption in a silicon photodiode," Opt. Lett. **29,** 1524–1526 (2004).
23. H. G. Winful, "Polarization instabilities in birefringent nonlinear media : apllication to fiber-optics devices," Opt. Lett. **11,** 33–35 (1986).
24. Q. Lin, J. Zhang, P. M. Fauchet, and G. P. Agrawal, "Ultrabroadband parametric generation and wavelength conversion in silicon waveguides," Opt. Express **14,** 4786–4799 (2006).
25. B. Cowan, "Optical damage threshold of silicon for ultrafastinfrared pulses ," Advanced accelerator concepts: 12th advanced accelerator concepts workshop. AIP conference proceedings, **877,** 837–843(2006).
26. Q. Lin, J. Zhang, G. Piredda , R. W. Boyd, P. M. Fauchet, and G. P. Agrawal, "Dispersion of silicon nonlinearities in the near infrared region," Appl. Phys. Lett. **91,** 021111 (2007).
27. S. Trillo, S. Wabnitz, W. C. Banyai, N. Finlayson, C. T. Seaton, G. I. Stegeman, and R. H. Stolen, "Observation of ultrafast nonlinear polarization switching induced by polarization instability in a birefringent fiber rocking filter," IEEE J. Quantum Electron. **25,** 104–112 (1989).
28. H. K. Tsang, C. S. Wong, T. K. Liang, I. E. Day, S. W. Roberts, A. Harpin, J. Drake, and M. Asghari, "Optical dispersion, two photon absorption and self-phase modulation in silicon at $1.5\mu m$ wavelength," Appl. Phys. Lett. **80,** 416–418 (1985).
29. H. Garcia and R. Kalyanaraman, "Phonon-assisted two-photon absorption in the presence of a dc-field: the nonlinear Franz-Keldysh effect in indirect gap semiconductors," J. Phys. B: Mol. Opt. Phys. **39,** 2737–2746 (2006).

1. Introduction

Silicon photonics has been widely viewed as a promising candidate for integration with microelectronics owing to silicon's high refractive index that enables one to scale the dimensions of silicon-based devices down to the size compatible with integrated-circuit processing [1–3]. As a result of the large third-order optical nonlinearity of silicon and tight optical confinement, silicon waveguides have been conjectured to provide a versatile platform for realization of a multitude of nonlinear optical functionalities [4, 5]. One of the distinguishing features of silicon as a semiconductor material – at least in certain spectral regions – is its pronounced linear and two-photon absorption (TPA), accompanied by the carrier generation. Generally, linear losses and TPA impose severe limitations on the silicon functionality for all-optical communications. Yet, several modalities have recently been proposed that essentially rely on TPA [6, 7]. To date, a number of fundamental advances have also been made in silicon photonics, including wavelength switching and generation, optical amplification and lasing, temporal soliton propagation and suprercontinuum generation, and dc field-induced suppression of the split-up of higher-order spatial vector solitons [8–17], to mention but a few examples. However, relatively little attention has so far been paid to the evolution of ultrashort pulse polarization inside silicon waveguides, and, to the best of our knowledge, the issue of the pulse polarization control has not been explored yet.

In this work, we describe theoretically and numerically the nonlinear polarization evolution of an ultrashort pulse, propagating in a silicon waveguide, subjected to the action of an external control electric field, which induces linear birefringence via the quadratic electro-optical

#102344 - $15.00 USD Received 6 Oct 2008; revised 12 Dec 2008; accepted 17 Dec 2008; published 29 Jan 2009

effect [18]. The polarization state of the pulse, transmitted through such a waveguide, is numerically simulated in the spectral interval extending from near- to mid-infrared. We have found that the transmitted pulse polarization can be controlled by adjusting the magnitude of the dc field as well as the input pulse power. Although the nonlinear polarization rotation and its applications are well known in the fiber optics context [19, 20], several new factors must be considered when the silicon waveguide is utilized. First of all, like any other semiconductor material, silicon has high linear loss and – in some spectral regions – pronounced nonlinear absorption that is also responsible for the free carrier generation. Second, the interplay of nonlinear absorption and controlled linear birefringence has lately been shown to lead to qualitatively new phenomena such as suppression of higher-order vector soliton breakup in silicon nanocrystal waveguides [17]. Further, silicon is known to have a sizable anisotropy of the nonlinear refraction [4]. At the same time, the anisotropy of silicon TPA is yet an open issue because of a discrepancy in reported optical and electrical measurements to date [21, 22]: The former appears to indicate that TPA is essentially isotropic, while the latter points in the other direction.

In this work, we will assume isotropic TPA since several aspects of the electrical measurements of Ref. [22] are yet to be clarified [4]. The pulse polarization dynamics is controlled by a static electric field, which is, in general, spatially inhomogeneous. We have discovered that despite very large linear losses, the nonlinear polarization instability regime – similar to the one encountered in lossless fibers – can be attained in the mid-infrared spectral region of silicon provided a special spatial profile of the controlled field is engineered.

This paper is organized as follows. In section (2), a theoretical model for the propagation of ultrashort light pulses of arbitrary polarization in low birefringent silicon waveguides subject to a controlling dc electric field is presented. In section (3), the results of numerical simulations of pulse shape and polarization control are presented and discussed. Section (4) summarizes concluding remarks.

2. Theory

Consider an optical pulse propagating in a planar waveguide filled with silicon. The pulse propagation is mediated by an electric field $\frac{1}{2}E_{ext}$ applied along the x-axis. The electric field of the pulse can then be represented as

$$\mathbf{E} = \frac{1}{2}[\mathbf{a}_x(\mathscr{E}_x e^{-i\omega t} + E_{ext}) + \mathbf{a}_y \mathscr{E}_y e^{-i\omega t}] + c.\,c. \tag{1}$$

Here the unit vectors $\mathbf{a}_x$ and $\mathbf{a}_y$ are assumed to be directed along [100] and [010] silicon crystal axes, respectively. The third-order dielectric susceptibility tensor of the silicon can then be represented as [4]

$$\chi^{(3)}_{ijkl} = \chi^{(3)}_{xxxx}[\frac{\rho}{3}(\delta_{ij}\delta_{kl} + \delta_{ik}\delta_{jl} + \delta_{il}\delta_{jk}) + (1-\rho)\delta_{ijkl}], \tag{2}$$

where i, j, k, l take on values x and y, and $\rho = 3\chi^{(3)}_{xxyy}/\chi^{(3)}_{xxx}$ is the nonlinear anisotropy coefficient; δ_{ijkl} is the Kronecker delta. The nonlinear polarization field, generated by any Kerr-type nonlinear medium, can be written as

$$P_{NL} = \varepsilon_0 \chi^{(3)} \vdots \mathbf{EEE}. \tag{3}$$

It follows from (1)– (3) that the component of the polarization tensor oscillating at the carrier frequency ω takes the form

$$\mathbf{P}_{NL} = \frac{1}{2}(\mathbf{a}_x \mathscr{P}_x + \mathbf{a}_y \mathscr{P}_y)e^{-i\omega t} + c.\,c., \tag{4}$$

#102344 - $15.00 USD Received 6 Oct 2008; revised 12 Dec 2008; accepted 17 Dec 2008; published 29 Jan 2009

where

$$\mathscr{P}_x = \frac{3\varepsilon_0}{4}\chi^{(3)}_{xxxx}\left[\left(|\mathscr{E}_x|^2+\frac{2\rho}{3}|\mathscr{E}_y|^2\right)\mathscr{E}_x+\frac{\rho}{3}\left(\mathscr{E}_x^*\mathscr{E}_y+12E_{ext}^2\mathscr{E}_x\right)\right], \tag{5}$$

and

$$\mathscr{P}_y = \frac{3\varepsilon_0}{4}\chi^{(3)}_{xxxx}\left[\left(|\mathscr{E}_y|^2+\frac{2\rho}{3}|\mathscr{E}_x|^2\right)\mathscr{E}_y+\frac{\rho}{3}\left(\mathscr{E}_y^*\mathscr{E}_x+4E_{ext}^2\mathscr{E}_y\right)\right]. \tag{6}$$

Here, we have assumed that ω lies well below any resonant frequency of the medium. It then follows that the third-order susceptibility is virtually independent of frequency in the vicinity of ω, so that $\chi^{(3)}(-\omega,\omega,\omega,-\omega)=\chi^{(3)}(-\omega,\omega,0,0)$, and, thus, one can use the same constant susceptibility to describe optical and electro-optical Kerr effects.

The nonlinear wave equation, governing beam propagation, can be cast into form

$$\nabla^2\mathbf{E}-\frac{1}{\varepsilon_0 c^2}\frac{\partial^2\mathbf{D}}{\partial t^2}=\mu_0\frac{\partial^2\mathbf{P}_f}{\partial t^2}+\mu_0\frac{\partial^2\mathbf{P}_{NL}}{\partial t^2}, \tag{7}$$

where

$$\mathbf{P}_f=\varepsilon_0\chi_f\mathbf{E}, \tag{8}$$

is the free carrier polarization field and $\mathbf{D}$ is the electric displacement. The free carrier induced linear susceptibility χ_f is given by the expression

$$\chi_f = 2n_0[n_f(N)+ic\alpha_f(N)/(2\omega)], \tag{9}$$

where n_o is the material refractive index, c is the speed of light in free space, $n_f(N)$ and $\alpha_f(N)$ are the free-carrier index change (FCI) and the free-carrier absorption (FCA) coefficients, respectively, and N being the number of free carriers.

In the usual slow-varying envelope approximation, the solution to (7) in the waveguide geometry can be sought in the form

$$\mathscr{E}_j(\mathbf{r},t)=F_j(x,y)u_j(z,t)e^{i\beta_{0j}z}, \tag{10}$$

where $F_j(x,y)$ is the spatial mode profile of the single-mode waveguide normalized such that $\int\partial x\partial y|F_j(x,y)|^2=1$; $u_j(z,t)$ are the slowly varying field amplitudes, and β_{0j} are the propagation constants of the components $j=x,y$. It follows that the wave equations for the slow-varying amplitudes can be represented as

$$\frac{\partial u_x}{\partial z}+\frac{i\beta_2}{2}\frac{\partial^2 u_x}{\partial\tau^2}=-\left(\frac{\alpha}{2}-i\sigma\right)u_x+4i\kappa u_x+i\gamma(|u_x|^2+\frac{2\rho}{3}|u_y|^2)u_x+\frac{i\gamma\rho}{3}u_x^*u_y^2e^{-2i\Delta\beta z}, \tag{11}$$

$$\frac{\partial u_y}{\partial z}+\frac{i\beta_2}{2}\frac{\partial^2 u_y}{\partial\tau^2}=-\left(\frac{\alpha}{2}-i\sigma\right)u_y+\frac{4i\kappa}{3}u_y+i\gamma(|u_y|^2+\frac{2\rho}{3}|u_x|^2)u_y+\frac{i\gamma\rho}{3}u_y^*u_x^2e^{2i\Delta\beta z}. \tag{12}$$

Here α is the linear loss coefficient; $\Delta\beta=\beta_{0x}-\beta_{0y}=\omega\Delta n/c$ and $\kappa=\frac{1}{2}\varepsilon_0\omega n_0 n_2 E_{ext}^2$ are the intrinsic and dc-field induced linear birefringence parameters,respectively, $\gamma=(n_2\omega/cA_{eff}+i\beta_{TPA}/2A_{eff})$, and n_2 and β_{TPA} being the nonlinear refractive index and the nonlinear absorption coefficient, respectively. Further, β_2 is the group velocity dispersion; $A_{eff}=(\int\partial x\partial y|F(x,y)|^4)^{-1}$ is the effective mode confinement area, $\beta_{1x}\approx\beta_{1y}=\beta_1$ is the inverse group velocity, and $\tau=t-\beta_1 z$ is retarded time. In deriving Eqs. (11) and (12), we assumed low birefringence of a silicon waveguide such that the parameter characterizing the free carrier contribution to linear refraction and absorption can be approximated by

$$\sigma\simeq\frac{n_0}{n}[\frac{\omega}{c}n_f+\frac{i}{2}\alpha_f], \tag{13}$$

#102344 - $15.00 USD Received 6 Oct 2008; revised 12 Dec 2008; accepted 17 Dec 2008; published 29 Jan 2009

where n is the mode refractive index. Here the FCI and FCA are given by the following empirical expressions [4]

$$n_f = -5.3\times 10^{-29}(\omega_r/\omega)^2 N, \quad \alpha_f = 1.45\times 10^{-21}(\omega_r/\omega)^2 N. \tag{14}$$

Here $\lambda_r = 2\pi c/\omega_r = 1550nm$.

Hereafter it will be more convenient to work in the circular polarization basis, defined by the transformation

$$u_1 = \frac{u_x e^{i\frac{\Delta\beta}{2}z} + iu_y e^{-i\frac{\Delta\beta}{2}z}}{\sqrt{2}} e^{-2i\zeta}; \qquad u_2 = \frac{u_x e^{i\frac{\Delta\beta}{2}z} - iu_y e^{-i\frac{\Delta\beta}{2}z}}{\sqrt{2}} e^{-2i\zeta}, \tag{15}$$

where $\zeta = \frac{4}{6}\varepsilon_0\omega n_0 n_2 \int E_{ext}^2(z)dz$. In the low birefringence limit, the wave equations in the circular polarization basis will take the form

$$\frac{\partial u_s}{\partial z} + \frac{i\beta_2}{2}\frac{\partial^2 u_s}{\partial \tau^2} = -\left(\frac{\alpha}{2} - i\sigma\right)u_s + i\kappa_{eff}u_{3-s} + \frac{i(3+\rho)\gamma}{6}(|u_s|^2 + 2|u_{3-s}|^2)u_s + \frac{i(1-\rho)\gamma}{2}u_{3-s}^2 u_s^*, \tag{16}$$

where $s = 1,2$ pertains to right 1 and left 2 circular polarizations, and the effective birefringence coefficient is defined as

$$\kappa_{eff}(z) = \frac{\Delta\beta}{2} + \frac{1}{2}\varepsilon_0\omega n_0 n_2 E_{ext}^2(z). \tag{17}$$

We model carrier generation by a phenomenological kinetic equation whose derivation relies on the following set of assumptions. First, we consider optical pulses much shorter than the characteristic carrier relaxation time, which implies virtually instantaneous response of the carriers to the input light intensity. Second, we assume a low repetition rate of the optical pulses such that each pulse interacts only with the carriers it has generated. Under these assumptions, the carrier density kinetic equation – which is a straightforward generalization of the one reviewed for linearly polarized pulses in Ref. [4] – can be shown to take the form

$$\frac{\partial N}{\partial t} = \frac{\beta_{TPA}(\omega)}{3A_{eff}^2 h\omega}\left[\frac{3+\rho}{4}(p_1+p_2)^2 + \frac{3+\rho+3(1-\rho)\cos 2\Delta\phi}{2}p_1 p_2\right], \tag{18}$$

where p_s and ϕ_s are the amplitude and phase, respectively, of the complex field u_s; $\Delta\phi = \phi_2 - \phi_1$.

Equations (13) – (18) govern the polarization dynamics of light pulses in silicon waveguides in the low birefringence approximation. In general, the light polarization evolution depends on the intricate interplay of a number of factors, including linear loss, TPA, nonlinear anisotropy, and externally controlled birefringence; a comprehensive picture can only be obtained via numerical simulations. Prior to presenting a detailed numerical analysis, however, we consider a quasi-CW input pulse and ignore the nonlinear anisotropy by assuming $\rho = 1$. Assume also that the input pulse carrier frequency lies in the spectral region where TPA is negligible. In this somewhat idealized case, the polarization dynamics is determined by a relative strength of linear losses and birefringence on the one hand, and the nonlinearity on the other. It follows that equations (16) for the slow-varying field amplitudes can be simplified as

$$\frac{\partial u_s}{\partial z} = -\frac{\alpha}{2}u_s + i\kappa_{eff}(z)u_{3-s} + \frac{2i\gamma}{3}(|u_s|^2 + 2|u_{3-s}|^2)u_s. \tag{19}$$

Further consider a special spatial profile for the electrostatic field such that

$$\kappa_{eff}(z) = \kappa_0 e^{-\alpha z}, \tag{20}$$

#102344 - $15.00 USD Received 6 Oct 2008; revised 12 Dec 2008; accepted 17 Dec 2008; published 29 Jan 2009

where κ_0 is constant. The corresponding dc field is given by the expression

$$E_{ext}(z) = \sqrt{\frac{2}{\varepsilon_0 \omega n_0 n_2}\left(\kappa_0 e^{-\alpha z} - \frac{\triangle\beta}{2}\right)}. \tag{21}$$

The controlling field in Eq. (21) can be realized in practice for any positive κ_0, provided $\Delta\beta < 0$. However, if the direction of the field coincides with the slow axis of the waveguide such that $\Delta\beta > 0$, one can realize the field distribution in Eq. (21) only if the field at the input to the waveguide is strong enough: $\kappa_0 \geq \frac{\Delta\beta}{2} e^{\alpha L}$. In the following, we assume that $\Delta\beta > 0$ and $\kappa_0 = \frac{\Delta\beta}{2} e^{\alpha L}$, and we rewrite Eq. (21) as

$$E_{ext}(z) = \sqrt{\frac{\Delta\beta}{\varepsilon_0 \omega n_0 n_2}\left[e^{\alpha(L-z)} - 1\right]}, \tag{22}$$

where L is the waveguide length.

With the exponential profile of the linear birefringence, it can be concluded by inspection that upon the scaling transformation

$$u(z) = e^{-\frac{\alpha}{2}z}\bar{u}(Z) \qquad\qquad Z = \frac{1-e^{-\alpha z}}{\alpha}, \tag{23}$$

the nonlinear wave equations (19) can be reduced to

$$\frac{\partial \bar{u}_s}{\partial Z} = i\kappa_0 \bar{u}_{3-s} + \frac{2i\gamma}{3}(|\bar{u}_s|^2 + 2|\bar{u}_{3-s}|^2)\bar{u}_s. \tag{24}$$

Equations (24) are formally equivalent to those governing the self-induced polarization rotation – and the polarization instability, resulting from a subtle balance between linear birefringence and self- as well as cross-phase modulation – in lossless birefringent optical fibers in a quasi-CW limit [19, 23]. Consequently, similar phenomena should take place in lossy silicon waveguides, provided the power of each polarization component of the pulse and the effective interaction length are scaled according to Eq. (23). It follows from Eqs. (20) and (23) that by choosing the electrostatic field profile decreasing at the rate determined by linear losses, one can accommodate the latter at the expense of shortening the effective interaction length. It should be stressed here that although we have so far ignored TPA and nonlinear anisotropy, the choice of the spatial profile of the controlling field given by Eq. (22), will prove to be crucial to realize instable polarization dynamics in the mid-infrared spectral region under general conditions.

3. Simulations and results

In our numerical simulations, we adopt a quasi-symmetric silicon-on-insulator (SOI) waveguide designed and studied in Ref. [24]. The effective cross-sectional area is taken to be $A_{eff} = 0.685\mu m^2$, and the group velocity dispersion (GVD) coefficients at $1550nm$ and $2300nm$ are estimated to be $\beta_2 \simeq 0$ and $\beta_2 = -1.3ps^2/m$, respectively. We point out here that the particular SOI design of Ref. [24] is chosen primarily for its low linear birefringence which enables the nonlinear polarization rotation to be realized at relatively small pulse intensities. The choice of the waveguide length and the magnitude of the linear birefringence coefficient is dictated by rather subtle considerations. On the one hand, the SOI waveguide must be long enough for the nonlinearity to significantly affect the polarization dynamics. On the other hand, the waveguide has to be sufficiently short to ensure that linear and nonlinear losses do not significantly attenuate the pulse intensity. Finally, the maximum operating value of the control field – which

#102344 - $15.00 USD Received 6 Oct 2008; revised 12 Dec 2008; accepted 17 Dec 2008; published 29 Jan 2009

determines effective linear birefringence – is limited by the electrical damage threshold of the material, equal to 30 V/μm for silicon [25]. We thus chose a suitable value of the linear birefringence coefficient for a maximum acceptable magnitude of the control field and then performed preliminary numerical simulations to find out the range of optimal waveguide lengths that would meet the rest of our requirements.

To characterize the field polarization state, we introduce the azimuth θ

$$\theta = \frac{1}{2}[\phi_1 - \phi_2]; \tag{25}$$

and the ellipticity parameter, defined as

$$e_p = \frac{\sqrt{p_1} - \sqrt{p_2}}{\sqrt{p_1} + \sqrt{p_2}}. \tag{26}$$

In the following simulations, we assume that a polarizer is placed at the waveguide exit. The polarizer is oriented such that if the waveguide length equals to the beat length due to linear birefringence, the lower input power is blocked. It can then be shown that the transmission coefficient, which is calculated generalizing the procedure developed in the fiber optical context [23], takes the form

$$T = \sqrt{\frac{p_1^2(L) + p_2^2(L)}{p_1^2(0) + p_2^2(0)}} \left\{ \frac{1}{2} - \frac{\sqrt{\frac{p_1(L)}{p_2(L)}}}{1 + \frac{p_1(L)}{p_2(L)}} \cos[\phi_1(0) - \phi_2(0) - \phi_1(L) + \phi_2(L)] \right\}, \tag{27}$$

p_s and ϕ_s are the power and phase, respectively, of the sth field component, $s = 1, 2$.

3.1. Mid-infrared spectral region

High nonlinear figure of merit (NFOM) of silicon material has been experimentally reported in the mid-infrared spectral region, i.e. for $\lambda = 2200 - -2400$ nm, where $n_2 \approx 1.5 \times 10^{-18}$ m^2/W, and $\beta_{TPA} \approx 0$ [26]. Due to the large optical nonlinearity and absence of TPA in silicon in this spectral region, we expect favorable conditions for the polarization instability to occur there, resulting in nontrivial polarization dynamics. Thus, we study numerically the polarization evolution of a 70 fs wide Gaussian pulse in the mid-infrared spectral range.

In Fig. (1) we display the transmission coefficient of the Gaussian pulse peak as the latter – having traversed a 6 mm long silicon waveguide – passes through the polarizer described in Eq. (27).

In these simulations, the strength of linear birefringence is determined by the value of the linear refractive index mismatch, $\triangle n = 2 \times 10^{-5}$. The input azimuth of the pulse is equal to $\pi/4$, and the pulse input ellipticity is zero. Further, the linear loss coefficient is such that $\alpha = 57.5 m^{-1}$, and the nonlinear anisotropy parameter of silicon is given by $\rho = 1.27$. The red line represents the transmission coefficient in the case of a mediated dc electric field equal to 25 V/μm, while the green line represents that in the absence of control field, $\frac{E_{ext}}{2} = 0$. The specifics of the control field spatial distribution along the waveguide are found to have no particular importance in this case. The degree of control over the pulse polarization in silicon waveguides – achieved despite linear losses by adjusting the electrostatic field – is manifest in Fig. (1) if one contrasts drastically different behaviors of the transmission coefficient as functions of the pulse power with and without the applied field.

To demonstrate the polarization control across the pulse temporal profile, we exhibit in Figs. (2) and (3) the shapes of the output Gaussian pulses as functions of the input pulse peak power for input azimuth $\theta = 75^o$.

#102344 - $15.00 USD Received 6 Oct 2008; revised 12 Dec 2008; accepted 17 Dec 2008; published 29 Jan 2009

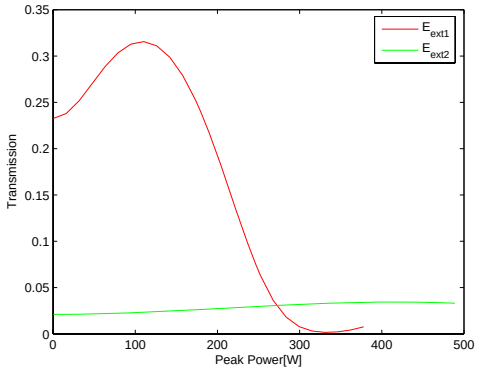

Fig. 1. Transmission coefficient as a function of the input peak power of a 70 fs long Gaussian pulse. The other parameters are: $e_{p0} = 0$, $\theta_0 = 45^o$, $\lambda = 2300nm$, $L = 6mm$, $\alpha = 57.5m^{-1}$, $\rho = 1.27$, $\frac{E_{ext1}}{2}$=25 V/μm and $\frac{E_{ext2}}{2} = 0$ V/μm. The linear refractive index mismatch is $\Delta n = 2 \times 10^{-5}$.

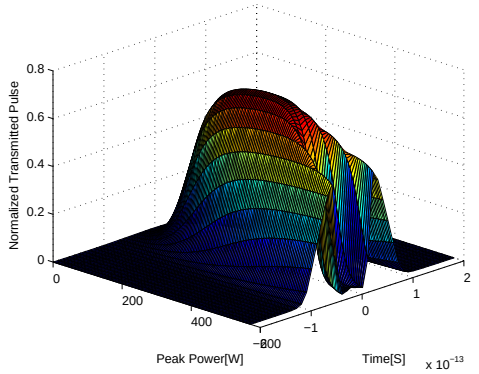

Fig. 2. Normalized transmitted pulse as a function of the input peak power. The input is a Gaussian pulse of the width $T_0 = 70$ fs. The other parameters are: $e_{p0} = 0$, $\theta_0 = 75^0$, $\lambda = 2300nm$, $\alpha = 57.5m^{-1}$, $L = 6mm$. The applied control field is $\frac{E_{ext}}{2} = 0$ V/μm.

#102344 - $15.00 USD Received 6 Oct 2008; revised 12 Dec 2008; accepted 17 Dec 2008; published 29 Jan 2009

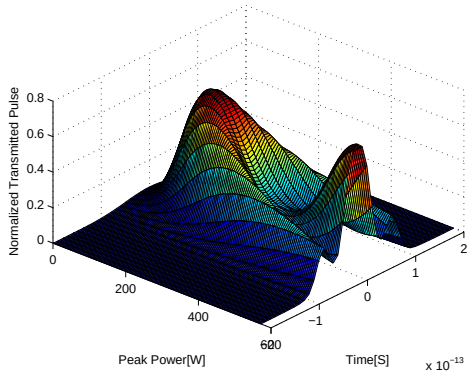

Fig. 3. Normalized transmitted pulse as a function of the input peak power. The input is a Gaussian pulse of the width $T_0 = 70$ fs. The other parameters are: $e_{p0} = 0$, $\theta_0 = 75^0$, $\lambda = 2300nm$, $\alpha = 57.5m^{-1}$, $L = 6mm$. The applied control field is $\frac{E_{ext}}{2} = 25\ \mathrm{V}/\mu\mathrm{m}$.

In Fig. (2), we depicted the results with no applied electric field, while the results in Fig. (3) correspond to the pulse propagation in presence of the homogeneous dc field, $\frac{E_{ext}}{2} = 25\ \mathrm{V}/\mu\mathrm{m}$, applied across the waveguide. It can be inferred from these figures that the pulse shape can also be readily controlled by influencing the pulse polarization state with the electrostatic field. We note that in this case the characteristic dispersion length is $L_D = 3.7mm$, which is shorter than the physical length of the waveguide; thus dispersion strongly influences the pulse reshaping and polarization dynamics.

In the same power range, the polarization instability is found to be taken place in sufficiently long waveguides. In Figs. (4)and (5)the simulation results for the pulse transmission through a $2-cm$ long silicon waveguide, followed by a polarizer oriented as before, are shown.

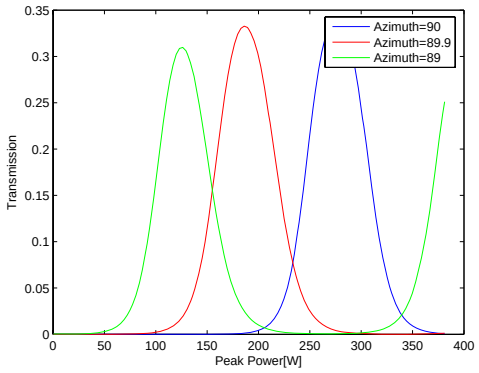

Fig. 4. Transmission coefficient as a function of the input peak power. The input is a Gaussian pulse of the width $T_0 = 70$ fs. The other parameters are: $e_{p0} = 0$, $\lambda = 2300nm$, $\alpha = 57.5m^{-1}$ and $L = 2cm$. The azimuth is chosen within the polarization instability regime. A properly designed spatial profile of the control field – given by Eq. (22) – is assumed, with the field magnitude at the entrance taken to be $25\ \mathrm{V}/\mu\mathrm{m}$.

Same waveguide and input pulse parameters as those in Fig. (1) are considered, except the azimuth is equal to $\pi/2$. In Fig. (5) a constant dc electric field, equal to $\frac{E_{ext}}{2} = 25v/\mu m$, is

#102344 - $15.00 USD Received 6 Oct 2008; revised 12 Dec 2008; accepted 17 Dec 2008; published 29 Jan 2009

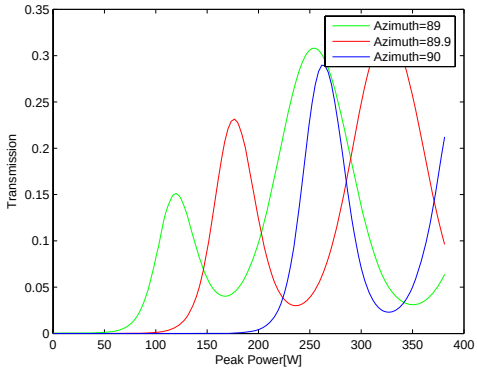

Fig. 5. Transmission coefficient as a function of the input peak power. The input is a Gaussian pulse of the width $T_0 = 70$ fs. The other parameters are: $e_{p0} = 0$, $\lambda = 2300nm$, $\alpha = 57.5m^{-1}$ and $L = 2cm$. The azimuth is chosen within the polarization instability regime. Constant electric field is assumed,i.e. $\frac{E_{ext}}{2} = 25\ \mathrm{V}/\mu\mathrm{m}$.

applied, while in Fig. (4) a spatially distributed field according to Eq. (22) control field is assumed with the maximum field at the waveguide input be equal to $25\ \mathrm{V}/\mu\mathrm{m}$. It can be seen in Figs. (4) and (5) that provided the waveguide is long enough, the polarization instability can occur – a small change of the input azimuth causes a considerable change in the transmission coefficient – regardless of the actual magnitude of the applied field. However, on comparing the cases of constant and exponentially decaying control fields, several instructive conclusions can be drawn. First of all, the instability is less pronounced – there is a lower sensitivity – in the former case than it is in the latter. Second, the pass bands occur at higher optical intensities in the former case than they do in the latter. Third and most important, the transmission bands overlap in the former case, and their shapes are somewhat irregular. In a sharp contrast, the polarization instability for the case of an exponentially distributed control field has the same regular qualitative features as its fiber optics counterpart [20]. The latter circumstance hints at possible applications of the appropriately electronically tailored polarization instability – with non-overlapping transmission bands, ideal for all-optical discrimination – to silicon-based ultra-high resolution devices [27]. In this parameter regime, the crucial role of the exponential control field distribution is attributed to a large waveguide length, which translates to high linear losses. As is shown in Section 2, the only way to accommodate such losses is for the field-induced linear birefringence to follow their profile which reduces the effective interaction length, but otherwise leaves the qualitative picture of the polarization instability unaffected.

3.2. Near-infrared spectral region

In this section, we study the pulse polarization dynamics at the telecommunication spectral wavelength, $1.55\mu m$. The silicon material, at $1.55\mu m$, has pronounced two photon absorption (TPA) such that nonlinear losses and the associated generated free carrier evolution must be taken into account [28]. On the other hand, on the application of the dc electrical field, the influence of the applied electrostatic field on the nonlinear absorption is known to be negligible [29].

In Fig. (6) we display the simulation results for the transmission coefficient of a Gaussian input pulse of the width $T_0 = 70$ fs as it passes through a polarizer at the exit of a $6 - mm$ long silicon waveguide. The other pulse and waveguide parameters are the same as those in Fig. (1).

The blue line represents the transmission coefficient in the case when all realistic effects are

#102344 - $15.00 USD Received 6 Oct 2008; revised 12 Dec 2008; accepted 17 Dec 2008; published 29 Jan 2009

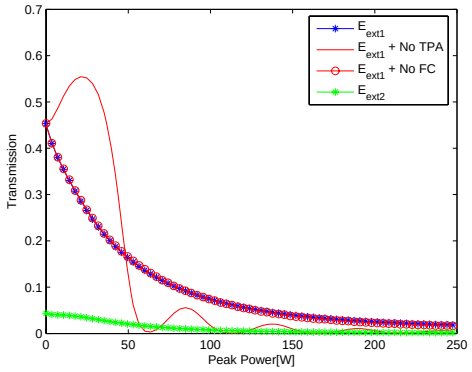

Fig. 6. Transmission coefficient as a function of the input peak power. The input is a Gaussian pulse of the width $T_0 = 70$ fs. The other parameters are: $e_{p0} = 0$, $\theta_0 = 90^o$, $\lambda = 1550nm$ and $L = 6mm$. Here $\frac{E_{ext1}}{2} = 25$ V$/\mu$m and $\frac{E_{ext1}}{2} = 0$ V$/\mu$m.

taken in to account, while the solid and circled red lines correspond to the cases of zero TPA and no generated free carries, respectively, which are presented for comparison. The constant electric field strength is taken to be 25 V$/\mu$m. As it can be seen from the Figure, the TPA affects the behavior of the transmission coefficient, much more significantly than does the free carrier generation. This is because, in this case, the nonlinear polarization rotation effects occur at relatively low power values such that the corresponding density of generated free carries is small. To illustrate the influence of the control field, we also present by the green line in Fig. (6) the transmission coefficient behavior in the absence of the control field.

Finally, we have carried out numerical simulations seeking polarization instability in this spectral region, only to have found out that the pass band was highly attenuated for the onset of the instability to be detectable. This is because the higher powers of the input pulses and/or longer waveguides are required to observe the polarization instability. Unfortunately, more intense pulses are greatly attenuated due to TPA which appears to extinguish any hope to attain the polarization instability regime.

4. Conclusions

We studied numerically the nonlinear polarization dynamics of ultrashort pulses in silicon waveguides in presence of a static controlling electric field. We have shown that polarization properties of such pulses can be easily tailored by simply adjusting the magnitude of the control field which would affect the strength of field-induced – via the quadratic electro-optic effect – linear birefringence of silicon. We have also found that despite the presence of strong linear losses, rather stringent requirements for realization of the polarization instability in silicon waveguides in the mid-infrared spectral region can be met, provided the special spatial profile – given by Eq. (22) – of the control field is engineered. Our simulations indicate that short silicon waveguides can serve as a viable platform for developing re-configurable all-optical and/or optically assisted electro-optical devices in the spectral range spanning from near to mid-infrared. Electrically re-configurable optical logic, pulse reshaping, switching and power dependant all-optical operations are among the silicon-based functionalities that appear to be promising.

#102344 - $15.00 USD Received 6 Oct 2008; revised 12 Dec 2008; accepted 17 Dec 2008; published 29 Jan 2009